

# ***1. Introduction***

## **1.1 Background**

Continuous increase in population and thereby increase in the demand for energy from all over the world is attracting the scientific community towards the search for a clean and reliable energy source. Nuclear energy can be a great solution as the proponents mark it as a clean, reliable, and sustainable energy source with reduced carbon emissions; and hence it can make a significant contribution to global energy needs [1].

Nuclear power generation is one of the most important and useful applications of nuclear reactors as it can moderately substitute fossil fuels. But, “If the spread of nuclear energy cannot be decoupled from the spread of nuclear weapons, it should be phased out”[2]. However, keeping the positive side on sight; researchers are trying to solve the concerns related to nuclear energy production. One of them is radioactive waste; by-products of the nuclear fuel cycle (NFC). The NFC operations involve the operation of the reactor, recycling of spent fuel, and fabrication of fuel, and producing nuclear waste which includes high, intermediate, and low-level radioactive waste (HLW, ILW, and LLW). Not only NFCs but also the nuclear power generation and other nuclear-related applications, for example, fusion and fission industry, defence programs, research, and agriculture produce nuclear radioactive waste as a by-product. To assure the tenable application of nuclear energy, it is pivotal to manage nuclear waste, specially HLW, securely and cogently. The HLW should be immobilized to ensure its safety for storage, transportation, and final repository disposal [3].

Preventing the dangers to the surroundings and ultimately to human beings from the exposure of nuclear HLW radioactive wastes, the ‘International Atomic Energy Agency’ (IAEA), expresses the declaration in (1995) which it handles the ethical and environmental issues associated with the disposal of nuclear wastes. *IAEA stated that the "Radioactive waste should be managed in such a way as to secure an acceptable level of protection for human health, provide an acceptable level of protection for the environment, assure that possible effects on human health and the environment beyond national borders will be taken into account, ensure that the predicted impacts on the health of future generations will not be greater than relevant levels of impact that are acceptable today and that the management practice will not impose undue burdens on future generations. Also, radioactive waste should be managed within an appropriate national legal framework including clear allocation of responsibilities and provision for independent regulatory functions, the generation of*

radioactive waste shall be kept to the minimum practicable, interdependencies among all steps in radioactive waste generation and management should be taken into account and the safety of facilities for radioactive waste management shall be appropriately assured during their lifetime" [4].

## 1.2 Types of Nuclear wastes

The main source of radioactive wastes is the nuclear fuel cycle (NFC) which includes high-level radioactive waste. These radioactive wastes are classified into three broad categories according to their radioactive content. These are defined as namely: (1) very low-level wastes (less than 400kBq/t of  $\beta$  and  $\gamma$  activity and can be eliminated with domestic waste), (2) low-level wastes (less than 4GBq/t of  $\alpha$  or 12Bq/t of  $\beta$  and  $\gamma$  activity), (3) intermediate-level wastes (contains activities more than low-level wastes, no heating effect of radioactive decay), (4) high-level waste (it contains the radioactive decay that produces ample heat which necessitates special design, storage, transport and disposal of waste).

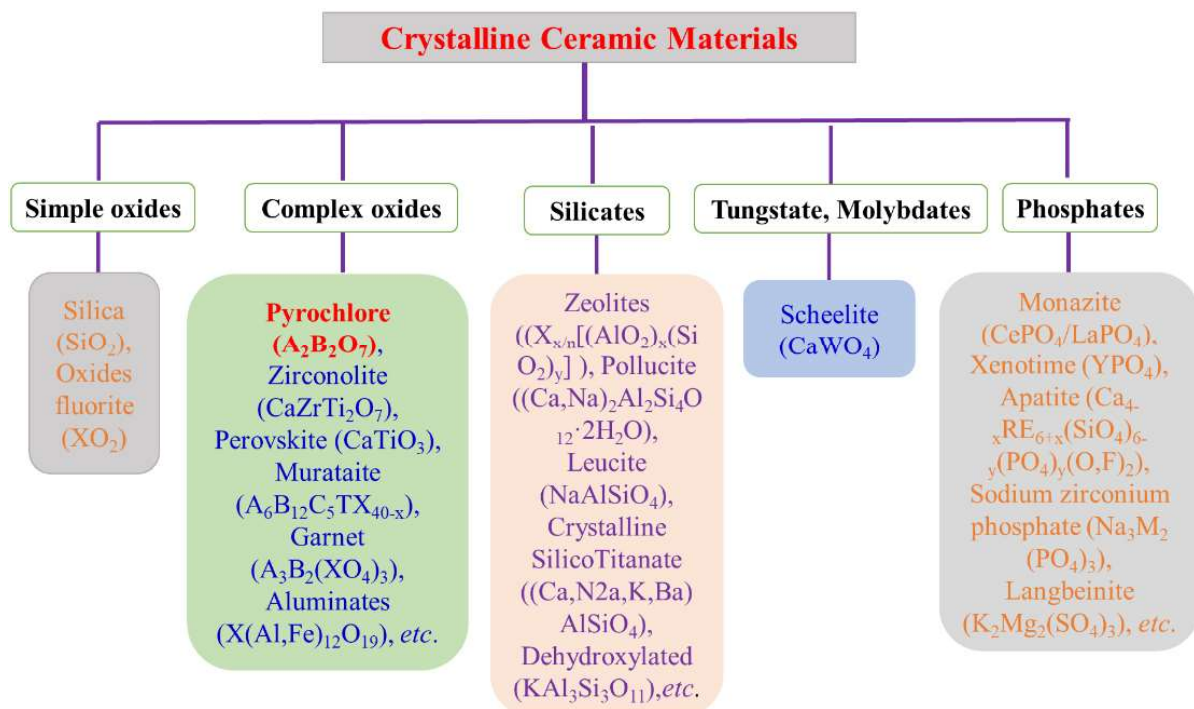


**Figure 1.1** The Classification of crystalline ceramic compounds as suitable waste forms for radioactive waste.

Among all these wastes high-level radioactive wastes need a special design for storage and disposal. The HLW wastes are hazardous and therefore needs proper management for immobilization [5,6]. Immobilisation of high-level radioactive wastes (HLWs) is achieved by incorporating the radioactive waste chemically into an appropriate matrix structure (typically

glasses or ceramics) to make it immobile and thus it is not able to escape into the environment [6,7]. To obtain the immobilization of HLW wastes, crystalline ceramics are found dominant for the current stage of modern nuclear technology development. Several types of ceramics have been designed with desired structures [8].

In 1953, Hatch introduced the idea of radioactive waste immobilization in the form of mineral phases [8]. The product of incorporating radionuclides into an appropriate host matrix is called the waste form. Thus, the waste form is considered as the initial barrier which prevents the escape of radionuclides into mother nature. Waste form prevents the uncork of radionuclides from compromised and breached containers due to human encroachment, corrosion, tremor, igneous invasion, and so on [3]. Therefore, choosing an appropriate waste form (host matrix) for immobilization of radioactive waste is not an effortless task and its stability in an extreme environment is not accepted as the solitary criterion. The challenges that are considered for selecting a waste form include, but are not limited to [6,9].

- (a) Ability to upload large radioactive waste.
- (b) Easy production of the system.
- (c) High radiation stability under environmental conditions.
- (d) possible upload of the mixture of radioactive nuclides and other pollutant species resulting in minimal secondary phases creation.
- (e) Must be agreeable with 'near field environment' of the waste geological repository and so on.

### **1.3 Crystalline ceramic host matrices for nuclear waste**

Ceramic materials based on different compositions were examined against the immobilization of radionuclide waste and actinides transmutations [8]. Based on the requirements, there are several forms of crystalline ceramics phase which have been utilized for radioactive waste immobilization. The Classification of crystalline ceramic compounds as suitable waste forms for the radioactive waste is presented in Fig. 1.1. The intent of the ceramics evolution was to emerge a waste form that must have superior physical, chemical, mechanical and thermal durability as compared to glass [10]. Among the ceramic crystalline compounds, a brief description of pyrochlore oxides has been discussed here which are chosen for research work in this thesis.

## 1.4 Pyrochlore oxides

The oxide compounds having the formula,  $A_2B_2O_7$  (where A and B are rare earth or trivalent metal ion and the transition or tetravalent metal ion respectively), constitute a family of isostructural phases to mineral pyrochlore. These compounds with more than 400 different combinations are predominantly ionic and cubic in nature due to the availability of broad-spectrum of elements substitution at both A site and B site [11–13]. Pyrochlore with the  $A_2B_2O_7$  stoichiometry provides an enormous band of structural and physical properties because of their numerous chemical compositions [11,12]. The pyrochlore according to its chemical composition may possess an insulating or metallic or semiconducting behavior. Pyrochlore oxides exhibit interesting piezo to ferroelectric, magneto-electric, and dielectric behaviors [11,14–17]. Numerous pyrochlore oxides are outstanding refractories while several Ln-containing pyrochlore oxides show fascinating phosphorescent and fluorescent behavior and feasibly can act as host materials for laser [18]. The defective (i.e., vacancy-containing) pyrochlores are considered oxygen electrodes due to their exceptional electronic and ionic conductivity [11,19]. Moreover, the pyrochlore oxides possess intrinsic oxygen (anion) vacancy which in turn makes them decent oxide-ionic conductors and probable candidates towards solid electrolytes for applications in moderate temperature solid oxide fuel cells (SOFCs) [18,19].

In particular, the  $A_2^{3+}B_2^{4+}O_7$  compounds have caught huge attention in the radioactive waste management field because of the capability of incorporating actinides, i.e., Th, U, and Np, etc. [11].

### 1.4.1 Structure of the pyrochlore oxides

The general representation of the oxide compounds belonging to the pyrochlore family can be described as  $A_2B_2X_6Y$  or  $A_2B_2O_6O'$ , where metal cations are situated at A and B site and anion situated at X and Y site. The pyrochlore,  $A_2B_2O_7$  is associated to  $Fd\bar{3}m$  space group as a superstructure of ideal fluorite ( $Fm\bar{3}m$ ) structure. Two different cation coordination polyhedrons are present in the pyrochlore oxide structure as depicted in Fig. 1.2. In the pyrochlore structure, the A-site cations sit at the 16d site and are correlated to eight oxygen atoms while the smaller B-site cations are co-ordinated to six oxygen atoms and occupy the 16c site. The anion sub-lattice has three different oxygen sites, out of the three, two sites belong to 8a and 48f positions, and the third site, 8b, is unoccupied. [20,21]. Hence, the ideal pyrochlore structure has ordered anion vacancies. The tetrahedrally coordinated anion site 8a is surrounded by cations situated at four A site; similarly, two A and B site cations surrounds

the 48f site such that there is a slight displacement from the center of the ideal tetrahedral to 8b site which is vacant. [20,21].

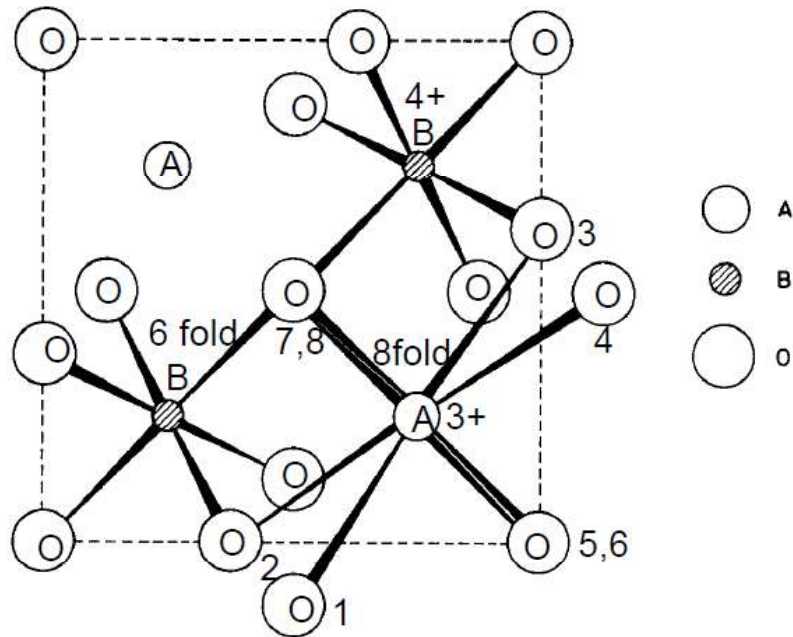


**Figure 1.2** Pyrochlore structure,  $A_2B_2O_7$ , exhibits the 8-fold coordination and 6-fold coordination polyhedron [12].

The phase transformation or structural change from pyrochlore to defect fluorite is caused by the cation anti-site defects i.e. exchange of atoms at A and B site and Frenkel defects [20].

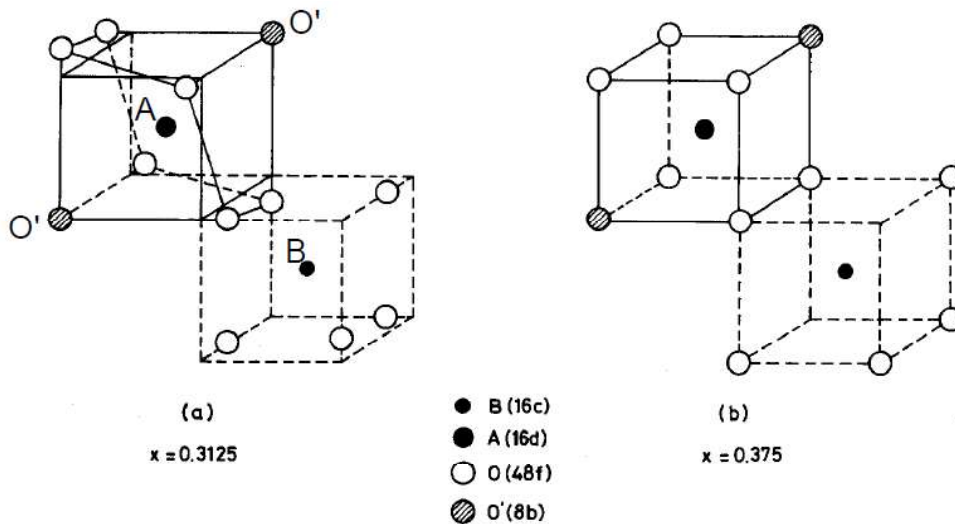


**Figure 1.3** The structural transition from pyrochlore structure  $A_2B_2O_6O'$  or  $A_2B_2X_6Y$  to ideal fluorite structure [12].

The fluorite and pyrochlore structures are nearly identical apart from the difference in the ordering of cations and anions [22]. The cationic radius ratio  $r_A/r_B$  decides the stability of the pyrochlore structure [23–29]. The cationic radius ratio must be in the limit  $1.46 < r_A/r_B < 1.78$  for the stable pyrochlore phase. If  $r_A/r_B$  ratio surpasses 1.78, the monoclinic structure is formed and the defect-fluorite structure is formed for a radius ratio below 1.46. The phase transformation from pyrochlore to fluorite structure becomes energetically favored with the decrement in  $r_A/r_B$  ratio. [24]. Although crystallization of many pyrochlore compositions is found to be in cubic structural form, a few pyrochlore structures were also found to be deviated from cubic symmetry to form rhombohedral, tetragonal, monoclinic, orthorhombic, and triclinic distortion structures [12].

### 1.4.2 $A_2^{3+}B_2^{4+}O_7$ pyrochlore oxides

According to the literature, there are several types of pyrochlore oxides family represented with  $A_2^{3+}B_2^{4+}O_7$ ,  $A_2^{3+}B_2^{5+}O_7$ ,  $A_2B_2O_6$ , and  $AB_2O_6$  [12].  $A_2^{3+}B_2^{4+}O_7$  formula is popularized among researchers due to the huge availability of  $A^{3+}$  and  $B^{4+}$  cations which possess the right cationic radius for the pyrochlore structure establishment. The pyrochlore compositions may be varied by putting any of the  $Lu^{3+}$  to  $La^{3+}$  elements on the  $A^{3+}$  site and any of the  $Ti^{4+}$  to  $Pb^{4+}$  elements on the  $B^{4+}$  site (as displayed in Fig.1.4). The realization and firmness of the pyrochlore structure are administrated by the  $r_A^{3+}/r_B^{4+}$  ionic ratio, and the oxygen parameter,  $X_{48f}$ .

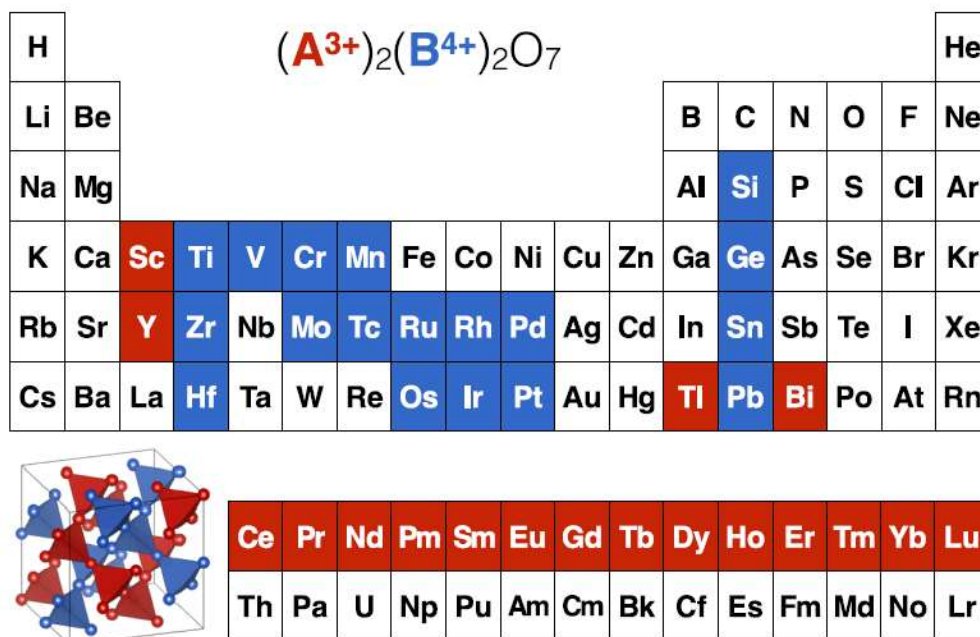


**Figure 1.4** The periodic table highlights elements with oxidation states 3+ (red) and 4+(blue) which may help to form the pyrochlore phase [30].

The ordered pyrochlores form when ionic radius ratio within the limit of  $1.46 \leq r_A/r_B \leq 1.78$  [11,12,31]. The composition forms a defect fluorite structure if the value is on the lower side of this range and if the value of  $r_A/r_B$  lies on the upper side then it forms a layered perovskite-type monoclinic structure [31]. The  $r_A/r_B$  value may be up to 2.3, if pyrochlore silicates and germinates are prepared at higher temperature as well as pressure. However, it is important to stress that in some cases in spite of using high pressure necessarily for pyrochlore (3+,4+) synthesis, the  $r_A/r_B$  may still be falling in the range 1.40-1.55 [12]. Also, in some cases, the formation of (3+,4+) pyrochlore oxides may be governed by the oxidation-reduction thermodynamic parameters [32]. A brief description of various pyrochlore oxides (based on the variation of elements on the B site) has been discussed here.

#### **1.4.2.1 Hafnate pyrochlores**

Functional Complex oxides of the  $A_2Hf_2O_7$  (A=La to Lu) series may exist either in the pyrochlore phase or fluorite phase depending on the sintering temperature and synthesis method [33]. complex oxide materials,  $A_2Hf_2O_7$  pyrochlore, have  $Fd\bar{3}m$  space group and they are closely associated with fluorite structure having  $Fm\bar{3}m$  space group. The hafnates series pyrochlore are important in many areas of scientific research. For example,  $Y_2Hf_2O_7$  transparent ceramics exhibits potential applications in nuclear medical fields related to high energy such as positron emission tomography (PET) and computed tomography (CT) [34]. In comparison to  $HfO_2$ ,  $La_2Hf_2O_7$  possesses a lower density of defects and low pinning of Fermi level which allows it to be considered as an ineluctable dielectric material [33]. The  $A_2Hf_2O_7$  system transparent ceramics was found to be promising materials for scintillator applications because of having a high density as well as the effective number [18].

#### **1.4.2.2 Ruthenate pyrochlores**

The compounds with general formula  $A_2Ru_2O_7$ , where A is Pr to Lu, Pb, Bi, Tl and Y are known as ruthenate pyrochlore. [35]. Ruthenate pyrochlore is found to have a color blue-black or black and the solid state reaction method can be used as an easy preparation method for them. Ruthenate has many important applications in scientific research areas. For example, Ruthenate in water electrolysis is observed to remain stable and active for OER. [36]. The inherited oxygen vacancy defects in ruthenate pyrochlore lead to improved activity of OER. [36]. The significant improvement in the performance of cells in comparison to  $RuO_2$  electrocatalysts concerning the stability and OER (Oxygen Evolution Reaction) activity in acidic medium is recently discovered for  $Y_2Ru_2O_{7-\delta}$ .  $Y_2Ru_2O_{7-\delta}$  demonstrates high resistance to the flow of electrons which results in high ohmic loss due to semiconducting characteristics

[35]. ( $A_2B_2O_{7-\delta}$ ) properties can further be engineered by doping A and/or B sites with desirable elements which may improve electrical conductivity and anion vacancies. [35,37]. It has been observed that  $Y_{1.85}Zn_{0.15}Ru_2O_{7-\delta}$  material's electrical conductivity is enriched by two orders of magnitude than  $Y_2Ru_2O_{7-\delta}$  at room temperature [35]. The hole doping effect can increase the number/amount of oxygen vacancies in these ceramic oxides, which may easily be attained by doping A site with 2+ cations. [37].

### 1.4.2.3 Iridate pyrochlores

The compounds having the formula,  $A_2Ir_2O_7$  (A=Pr-Lu, Y, Bi, and Tl) are known as iridate pyrochlore and it can easily be synthesized via the solid-state method [12]. The single crystals of iridate pyrochlore can be grown via flux techniques or vapor transport. The spin-orbit coupling (SOC) effect gets much pronounced in 5d- based iridium pyrochlore due to its high atomic number [12,38]. Moreover, 5d orbitals have comparatively feebler electronic correlation and therefore, the 5d based materials manifest a cognate scale among relevant energies i.e. spin-orbit coupling, electronic correlation, and crystal field effect.  $A_2Ir_2O_7$  Pyrochlore has an interesting arrangement of structure in which A and Ir atoms share the corner, resulting in an interpenetrating tetrahedral shape. This arrangement gives rise to new physics caused by induced geometrical frustration due to the particular positioning of atoms [37]. Iridate pyrochlore's physical characteristics may vary from magnetic insulating to paramagnetic metallic phase depending on the choice of A-site cation, However, antiferromagnetic (AFM) insulating phase is manifested by them at low temperature [39]. It is also interesting to know about the  $Y_2Ir_2O_7$  pyrochlore which has  $Y^{3+}$ , a non-magnetic element, therefore realizing that the Ir sub-lattice mostly governs the magnetic properties [38].

### 1.4.2.4 Stannate pyrochlores

Stannate pyrochlore compounds,  $Ln_2Sn_2O_7$  (Ln=La, Y, Pr-Yb) have a cubic structure ( $Fd\bar{3}m$ ). Owing to remarkable properties (e.g., high catalytic activity, ease of defects formation, high thermal stability, *etc.*) and emerging applications in different areas such as metal-semiconductor transitions, colossal magnetoresistance magnetic frustration/spin ices, superconductivity, mixed conductivity ferroelectrics, catalysis, and pigments established it as technologically suitable compound [12,40,41]. Ting et al. prepared the  $Ln_2Sn_2O_7$  (Ln=Y, La, Pr-Yb) compounds using a simple and economical hydrothermal method at the relatively low temperature, i.e., 200°C [40]. They found that the A-site cations play an important role in the infrared and Raman vibrational spectra of stannate pyrochlores. The peak position of vibrational modes altered with the cationic radius of  $Ln^{3+}$  [40]. Using appropriate trivalent

oxides, Lian et al. prepared the stannate pyrochlores, and Rietveld refinement of powder neutron and synchrotron XRD data was performed to investigate the associated structural properties [23]. Moreover, the high-temperature oxide melt solution calorimetry was employed to determine the enthalpies of the series of the stannate pyrochlores. As the radius of the cation at the A-site declines, the enthalpy of binary oxides of  $\text{Ln}_2\text{Sn}_2\text{O}_7$  becomes further endothermic. The enthalpy has been reported to be more exothermic with the increase of A-sites ions [23].

Further, in-situ transmission electron microscopy (TEM) was accustomed to evaluate the radiation effect of these stannate pyrochlores when exposed to 1 MeV  $\text{Kr}^{2+}$  ions at the temperature ranging from 25 to 1000 K. In-situ TEM study reveals that with the upsurge in irradiation temperature, the critical amorphization dose upsurges alike due to energetic annealing impact becoming more efficacious in reinstating the crystallinity. The critical temperature  $T_c$  was found to be  $\sim 960$  K for  $\text{La}_2\text{Sn}_2\text{O}_7$ , 700 K for  $\text{Nd}_2\text{Sn}_2\text{O}_7$ , and 350 K for  $\text{Gd}_2\text{Sn}_2\text{O}_7$ . These results indicated that the radiation resistance of stannate pyrochlores varies immensely with the variation of composition and temperature [23]. It was found that after being ion irradiated at ambient temperature and 25 K using a dosage of 6.82 dpa,  $\text{Er}_2\text{Sn}_2\text{O}_7$  and  $\text{Y}_2\text{Sn}_2\text{O}_7$  demonstrated greater "resistance" to amorphization, and amorphization had no signs in the observation. All irradiated stannate pyrochlores experienced a phase transformation from pyrochlore to fluorite structure, similar to titanate and zirconate pyrochlores [42–45]. As the cationic proportion,  $r_{\text{Ln}^{3+}}/r_{\text{Sn}^{4+}}$  declines from 1.68 to 1.526 for  $\text{La}_2\text{Sn}_2\text{O}_7$  and  $\text{Gd}_2\text{Sn}_2\text{O}_7$  respectively, the threshold temperature ( $T_c$ ) required to amorphize, declines from 960 K to 350 K, implying a much improved defect recovery capability of  $\text{Gd}_2\text{Sn}_2\text{O}_7$  [23].

It is worth mentioning that the stannate pyrochlores possess substantially higher critical amorphization temperatures than  $\text{Ln}_2\text{Ti}_2\text{O}_7$  and  $\text{Ln}_2\text{Zr}_2\text{O}_7$  pyrochlores with similar cationic ratios. For instance,  $\text{La}_2\text{Sn}_2\text{O}_7$  and  $\text{Y}_2\text{Ti}_2\text{O}_7$  have a cation radii ratio of 1.68; despite that the threshold amorphization temperature is 960 K and 780 K for  $\text{La}_2\text{Sn}_2\text{O}_7$  and  $\text{Y}_2\text{Ti}_2\text{O}_7$  respectively upon irradiation of 1 MeV  $\text{Kr}^{2+}$  [23]. Moreover, although the cationic ratio of  $\text{Nd}_2\text{Sn}_2\text{O}_7$  (1.607) is slightly less than that of  $\text{Lu}_2\text{Ti}_2\text{O}_7$  (1.61), the threshold temperature of  $\text{Nd}_2\text{Sn}_2\text{O}_7$  (700 K) is considerably larger than  $\text{Lu}_2\text{Ti}_2\text{O}_7$  (480 K). Further, the cationic ratio of  $\text{Gd}_2(\text{Zr}_{0.75}\text{Ti}_{0.25})_2\text{O}_7$  ( $\sim 1.526$ ) is similar to  $\text{Gd}_2\text{Sn}_2\text{O}_7$  ( $\sim 1.526$ ), but there is an intense difference in the radiation tolerance. Surprisingly,  $\text{Gd}_2\text{Sn}_2\text{O}_7$  becomes amorphized at  $\sim 3.4$  dpa given at room temperature while even after ion irradiation at 25 K,  $\text{Gd}_2(\text{Zr}_{0.75}\text{Ti}_{0.25})_2\text{O}_7$  does not show amorphization [23]. This more complicated conduct of stannate pyrochlores could be explained by differences in cation electrical configurations and bond type. Here, it should be noted that

the bond Sn-O in stannate pyrochlores has a smaller extent of deformation and favoured the ordered pyrochlore superstructure [46]. The Sn-O bond in  $\text{Ln}_2\text{Sn}_2\text{O}_7$  seems to be far covalent than the B-O bonds observed in  $\text{A}_2\text{Ti}_2\text{O}_7$ ,  $\text{A}_2\text{Zr}_2\text{O}_7$ , and  $\text{A}_2\text{Hf}_2\text{O}_7$  [47]. Therefore, in comparison to titanate and zirconate pyrochlores with alike cationic ratios, the stannate pyrochlore is better susceptible to ion irradiation caused amorphization.

#### 1.4.2.5 Titanate pyrochlores

Rare-earth titanates,  $\text{A}_2\text{Ti}_2\text{O}_7$ , where A= a rare earth element, have gained the attraction of researchers due to remarkable chemical durability. The utilization of titanate pyrochlore as probable host matrices for radioactive wastes is still being studied. [48]. Because of their diverse and usually unorthodox magnetic ground states, the magnetic properties of titanate pyrochlores are of interest [49]. Irradiation-induced lattice swelling in  $\text{Lu}_2\text{Ti}_2\text{O}_7$  can be explained by the creation of cation anti-site defects, according to Li et al. [50]. The exchange of atomic positions within the sub-lattice of A and B cation is known as antisite defect and it can be represented as  $\text{A}_\text{A}+\text{B}_\text{B} \rightarrow \text{A}_\text{B}+\text{B}_\text{A}$ . According to the previous studies, the titanate pyrochlores ( $\text{Ln}_2\text{Ti}_2\text{O}_7$ ) seem less resistant to radiation-induced amorphization than zirconates ( $\text{Ln}_2\text{Zr}_2\text{O}_7$ ) [24,51]. The reason for this is that the zirconates may easily facilitate disorder (especially anti-site defects) than titanate pyrochlore. Ewing et al. observed that due to vital annealing effects, the critical amorphization fluence in titanate pyrochlores upsurges with rising temperature. The critical amorphization fluence becomes infinity beyond the critical amorphization temperature ( $T_c$ ), and total amorphization cannot occur. To assess the radiation resistance of materials in high radiation exposures, the critical amorphization dose at ambient temperature or 25 K can be utilized.

Moreover, there can be a large uncertainty in determining the critical amorphization fluence for titanate pyrochlore because of the low ion fluence requirement towards total amorphization [52]. When the amount of ion irradiation created defects surpasses critical amorphization dose because of collision cascade overlap, total amorphization may take place. [53]. Wen et al. investigated the radiation resistance of nanocrystalline (NCs)  $\text{A}_2\text{Ti}_2\text{O}_7$  (A=Gd, Ho and Lu) upon irradiation of 1-MeV  $\text{Kr}^{2+}$  ions [54]. They observed that coarse-grained counterparts of nano-crystalline titanate pyrochlore have lower critical amorphization fluence at ambient temperature which signifies a better amorphization tolerance for nano-crystalline. Sattonnay et al. stated that the  $\text{RE}_2\text{Ti}_2\text{O}_7$  compounds became amorphized easily when low-energy ion irradiation was used. The critical/threshold temperature,  $T_c$ , rises with a growing radius of the A-site cation, implying the substantial role of the A-site cation [28]. Furthermore,

Wang et al. observed that a comparatively low dose of 0.2 dpa was enough to amorphize  $\text{Gd}_2\text{Ti}_2\text{O}_7$  at ambient temperature and 1100 K was found to be the ‘critical temperature’ [43]. Zhang et al. investigated that the defects production hang on the pressure and phase stability in  $\text{Gd}_2\text{Ti}_2\text{O}_7$  [55]. The structural durability of materials undergoing an order-disorder phase transition is influenced by pressure. At very high pressures ( $>50$  GPa), pyrochlore undergoes order-disorder transformation and amorphization, as studied by previous researchers [56,57]. Yang et al. examined the significance of ion species in radiation tolerance of  $\text{Lu}_2\text{Ti}_2\text{O}_7$  against ion irradiation with three different ion beams, i.e., 400 keV  $\text{Ne}^{2+}$ , 2.7 MeV  $\text{Ar}^{11+}$ , and 6.5 MeV  $\text{Xe}^{26+}$  [58]. During these irradiation experiments, the radiation effects i.e. amorphization/phase transformation and change in lattice parameter in  $\text{Lu}_2\text{Ti}_2\text{O}_7$  manifest a pronounced dependence on the implanted ion elements. Choice of energy and implanting ion affects the critical amorphization dose. Therefore,  $\text{Lu}_2\text{Ti}_2\text{O}_7$  becomes more prone to irradiation effects i.e. lattice swelling and amorphization upon heavy ion irradiation. Here, it is worth mentioning that upon low fluence high-energy-irradiations, only a few fractions of dpa are required for defect fluorite transition of the titanate pyrochlore followed by amorphization [58]. The zirconate pyrochlore, contrarily, favored order-disorder transformation, resulting in a defect-fluorite structure that can withstand an immensely high irradiation dose ( $>100$  dpa) [44].

#### **1.4.2.6 Zirconate pyrochlores: Material of interest**

Zirconate pyrochlore compounds,  $\text{Ln}_2\text{Zr}_2\text{O}_7$  ( $\text{Ln}=\text{La-Gd}$ ) can be synthesized simply by the solid-state method and it possesses a cubic structure [12]. Fig. 1.5 depicts a schematic of the structure of the ordered pyrochlore.  $\text{Ln}_2\text{Zr}_2\text{O}_7$  pyrochlore exhibit a broad spectrum of remarkable properties for example high ionic conductivity, chemical stability, high radiation stability, high thermal, and excellent thermal stability [12,59–65].

These inevitable properties of the  $\text{Ln}_2\text{Zr}_2\text{O}_7$  pyrochlore oxides established them an appropriate aspirant for the important technological applications, for example, high-temperature superconductors, piezoelectricity, photoluminescence, immobilization of radioactive nuclear waste, catalysis, thermal barrier coatings, high-temperature solid oxide fuel cells, solid electrolytes, spin liquids, and so on [63–65]. It should be noted that the properties of the  $\text{Ln}_2\text{Zr}_2\text{O}_7$  compounds significantly depend on the structural ordering/ disordering and defects irradiation, temperature, or pressure. Paul et al. prepared the  $\text{La}_2\text{Zr}_2\text{O}_7$  and investigated the effect of annealing temperature on phase transition (order-disorder) in the system.

They reported that the XRD, Raman spectroscopy, and TEM analysis reveal the disordered fluorite to pyrochlore phase transformation in  $\text{La}_2\text{Zr}_2\text{O}_7$  between 1000 and 1450°C

[66]. The  $\text{La}_2\text{Zr}_2\text{O}_7$  acts as a brilliant proton conductor by suitably doping both the cation sites (La and Zr) [67].  $\text{La}_2\text{Zr}_2\text{O}_7$  pyrochlore with notably high proton conductivity may be considered as propitious materials for sensing and solid oxide fuel cells employments. [67,68]. The engineering of the proportional presence of pyrochlore and defect fluorite phase i.e. order-disorder ratio in  $\text{La}_2\text{Zr}_2\text{O}_7$  was performed by Ou et al. via annealing temperature control.

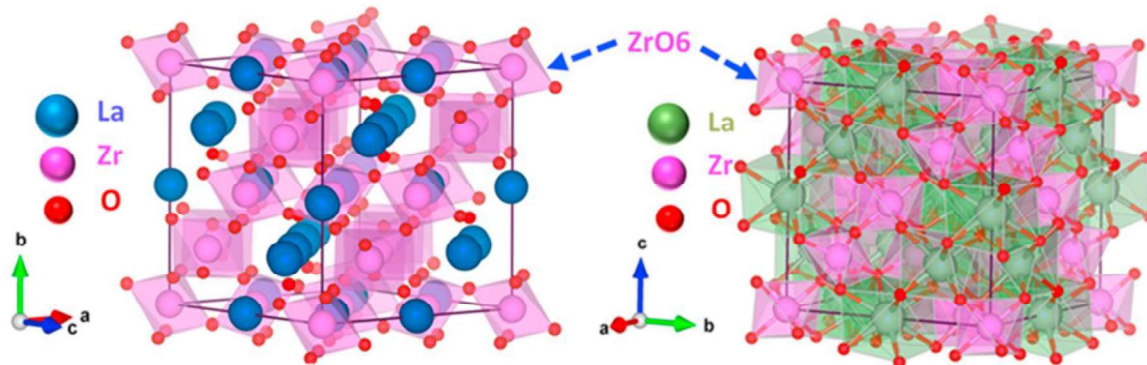


**Figure 1.5** Representation of the crystal structure of  $\text{La}_2\text{Zr}_2\text{O}_7$  pyrochlore. The magenta and light green are  $\text{ZrO}_6$  trigonal antiprisms and  $\text{LaO}_8$  cubes or scalenohedra.

The mixed-phase  $\text{La}_2\text{Zr}_2\text{O}_7$  was found to have superior conductivity on account of lattice mismatch at the interface joining pyrochlore and defect fluorite phase. [68]. Chartier et al. published that owing to low anti-site defect formation energy i.e.  $\sim 2$  eV, lanthanum zirconate is highly inclined to cation disorder formation [69]. Therefore, attributing to the simplicity of order-disorder transition,  $\text{La}_2\text{Zr}_2\text{O}_7$  must be extremely tolerant to radiation effects. However, when exposed to a 1.5 MeV  $\text{Xe}^+$  ion through a dosage of 5.5 dpa at ambient temperature,  $\text{La}_2\text{Zr}_2\text{O}_7$  exhibits poor characteristics of radiation resistance and becomes amorphized [44]. Previous studies suggest that  $\text{La}_2\text{Zr}_2\text{O}_7$  is admirable for immobilization of actinide (Pu can be fused at any of the cationic sites) wastes [70,71].

Zhang et al. used isothermal annealing at different temperatures (1100-°1550C) to prepare  $\text{Gd}_2\text{Zr}_2\text{O}_7$  possessing variable degrees of cation disorder. The degree of cation order in  $\text{Gd}_2\text{Zr}_2\text{O}_7$  grows with the upsurging temperature [20].  $\text{Gd}_2\text{Zr}_2\text{O}_7$  exhibits the phase transformation to a disordered defect-fluorite structure without amorphization even after applied pressure of 44 GPa [55].

In the last few decades, a considerable number of researches have been undertaken on the feasibility and characteristics of  $\text{Gd}_2\text{Zr}_2\text{O}_7$  pyrochlore as a waste form for HLW. [27,43,59,60,72–75]. Ion-beam irradiations with energies varying from few keV to few MeV have been used to reproduce alpha-decay damage in a broad spectrum of pyrochlore compositions, particularly in  $\text{A}_2\text{Zr}_2\text{O}_7$  and  $\text{A}_2\text{Ti}_2\text{O}_7$  systems, in ion beam irradiation the incident

ions produce interstitial atoms cascade and vacancies because of an incident ion and lattice structure's elastic collision [44,45,76].

Several SHI irradiations (energy range: MeV to GeV) researches were performed by Patel et al., Lang et al., and Sattonnay et al. and they reported that order-disorder transformation and amorphization induced by irradiation intensely rely on elemental composition [27,28,72,76,77]. These outcomes also show that the titanate pyrochlore is greatly susceptible to transformation caused via irradiation, i.e., titanate pyrochlore ( $Gd_2Ti_2O_7$ ) became amorphized at comparatively low dosage  $\sim 0.2$  dpa at ambient temperature. However, the  $Gd_2Zr_{2-x}Ti_xO_7$  shows consistent enhancement in “resistance” to ion beam-induced amorphization with increased Zr content, and hence, the phase transformation is favored towards a disordered, defect-fluorite phase. After the maximal irradiation, the end member,  $Gd_2Zr_2O_7$ , which originally consists of a mixture of crystalline pyrochlore and defect-fluorite structure, is altered to the disordered, defect-fluorite structure with no signs of amorphization.

Moreover, to examine the impact of nuclear collisions and electronic excitations, Sattonnay et al. synthesized pellets for  $Gd_2(Ti_{2-x}Zr_x)O_7$  composition and bombarded through heavy ions having energies varying from few MeV to few GeV [77]. The resistance to amorphization produced by irradiation decreases with increasing Zr engrossment at low energy (4 MeV Au ions).  $Gd_2Ti_2O_7$  is amorphized easily, but  $Gd_2Zr_2O_7$  goes through the transition to a disordered fluorite structure. Similar results have been obtained with significantly lower ion fluences for high energy irradiations (through 1.5 GeV Xe or 2.6 GeV U ions).

In accordance to preliminary calculations, experiments, and a variety of crystal structures ranging from pyrochlore to disordered fluorite structure, the  $Gd_2Zr_2O_7$  oxide seems to be a promising candidate for hostile environments in the interest of safe and effective management of radioactive wastes and surplus actinides.

## 1.5 Motivation

There is a necessity for safe and effective management of hazardous and environmentally sensitive high-level radioactive wastes (HLWs). Materials used for effective management of (involving their safe discharge and storage) radioactive wastes should be stable in radioactive environments [7]. Therefore, the development of radiation-resistant compounds for the effective management of radioactive wastes is of utmost importance.

Several organizations from around the world are working to find an appropriate matrix for the secure burial of radioactive waste [7,78]. For this reason, a variety of materials such as glasses, cement, ceramics, and others are being examined by various researchers around the globe [6].

The disadvantage of borosilicate glass is that it has an inclination towards devitrification in the company of water and vapor at high pressure and high temperature, which could occur after disposal in a geological repository [2]. Furthermore, intrusion of water into geological repositories might result in the creation of water-soluble salts, which can increase the few species' leachability.

Furthermore, fixing actinides and other radioactive wastes in ceramic matrix offers various advantages, including increased thermodynamic durability, low leachability, and improved chemical stability and radiation tolerance [8].

Based on the findings of the literature review, zirconate pyrochlores are cogitated to be significant host matrices for radioactive waste incorporation.

## 1.6 Scope and Goals of Thesis

The main aspiration of this thesis is to present the research work carried out on selected zirconate pyrochlores, i.e.,  $\text{La}_2\text{Zr}_2\text{O}_7$  and  $\text{Gd}_2\text{Zr}_2\text{O}_7$ . The effect of annealing temperature and ion irradiation on the structural modifications of  $\text{La}_2\text{Zr}_2\text{O}_7$  has been discussed as a pyrochlore structure,  $\text{La}_2\text{Zr}_2\text{O}_7$  has a broad spectrum of applications, including photoactive composites, catalysts, and thermal barrier coatings [70,79]. The impact of different degrees of structural defects on the radiation tolerance of  $\text{Gd}_2\text{Zr}_2\text{O}_7$  samples was investigated upon swift heavy ion irradiation (100 MeV  $\text{I}^{7+}$ ) and evaluated the capabilities of  $\text{Gd}_2\text{Zr}_2\text{O}_7$  samples for the possible applications in hostile environments such as radiation tolerant hosts for safe and effective management of radioactive nuclear wastes and surplus actinides

## 1.7 Thesis objectives

The precise objectives of the research work plans are categories as follows:

- Effect of annealing temperature on structural properties of  $\text{La}_2\text{Zr}_2\text{O}_7$  pyrochlore.
- Structural modifications of  $\text{La}_2\text{Zr}_2\text{O}_7$  pyrochlore upon irradiation with MeV ions.
- Order-disordering engineering in  $\text{La}_2\text{Zr}_2\text{O}_7$  pyrochlore upon irradiation with keV ions.
- Role of structural ordering on the radiation resistance response of  $\text{Gd}_2\text{Zr}_2\text{O}_7$  pyrochlore.
- Investigation of high electronic excitation induced structural modifications of  $\text{Gd}_2\text{Zr}_2\text{O}_7$  pyrochlore.

## 1.8 Structure of the Thesis

After the achievement of the aforementioned objectives, we have integrated the results with respective discussions in five different chapters (i.e. Chapter 3 to Chapter 7) confined between the introduction (Chapter 1) followed by synthesis process and experimental techniques (Chapter 2) and a conclusion chapter (Chapter 8).

**Chapter 1**, entitled “Introduction” presents a brief description of the contribution of the pyrochlore oxides in the field of various technological applications, where the prime focus is given on  $A_2^{3+}B_2^{4+}O_7$  pyrochlore.

**Chapter 2**, entitled “Synthesis methods and experimental techniques” provides the details of the synthetic methodology and irradiation experiments. A brief review of the various analytical characterization tools is also summarized.

**Chapter 3**, entitled “Impact of annealing temperature on structural and microstructural properties of  $La_2Zr_2O_7$  pyrochlore” describes the assessment of structural ordering as a function of annealing temperature.

**Chapter 4**, entitled “Structural response of  $La_2Zr_2O_7$  pyrochlore upon irradiation with 1.0 MeV  $Xe^{4+}$  ions” presents the irradiation temperature and ion fluence dependent structural modifications of  $La_2Zr_2O_7$  pyrochlore.

**Chapter 5**, entitled “Investigation of atomic order-disorder in the  $La_2Zr_2O_7$  pyrochlore under low energy (500 keV,  $Kr^{2+}$ ) ion irradiation” demonstrates the involvement of the  $x_{48f}$  parameter in the enhancement of disordering in the system.

**Chapter 6**, entitled “Role of structural ordering on the radiation resistance response of  $Gd_2Zr_2O_7$  pyrochlore” exhibits that the structural ordering/disordering plays a pivotal role in the radiation resistance engineering of  $Gd_2Zr_2O_7$  pyrochlore

**Chapter 7**, entitled “Structural modification of  $Gd_2Zr_2O_7$  pyrochlore induced by swift heavy ions for nuclear waste immobilization” demonstrates that the structural defects enhanced as a function of ion fluence.

**Chapter 8**, entitled “Summary and Conclusions” summarizes the overall concluding remarks drawn from the thesis by justifying its title and proposed objectives. This chapter also highlights the probable scope of outspreading this work in the near future.

## References

- [1] A. Pal, B.P. Mandal, K.A. Dubey, D. Jain, A. Bedar, A. Kumar, N. Goswami, B.C. Nailwal, B.N. Rath, A.K. Debnath, A.K. Singha, N.N. Kumar, R.D. Jain, A.K. Tyagi, R.C. Bindal, S. Kar, Polysulfone-Gd<sub>2</sub>Zr<sub>2</sub>O<sub>7</sub> mixed-matrix membranes with superior radiation resistant properties: Fabrication and application of a membrane device for radioactive effluent treatment, *Chem. Eng. J. Adv.* 1 (2020) 100006. <https://doi.org/10.1016/j.ceja.2020.100006>.
- [2] M.R. Greenberg, *Nuclear waste management, nuclear power, and energy choices*, 2012. <https://doi.org/10.1007/978>.
- [3] Hyatt, Ojovan, Special Issue: Materials for Nuclear Waste Immobilization, *Materials (Basel)*. 12 (2019) 3611. <https://doi.org/10.3390/ma12213611>.
- [4] R.A. Rahman, *Radioactive Waste*, InTech, 2012. <https://doi.org/10.5772/1859>.
- [5] M.I. Ojovan, W.E. Lee, S.N. Kalmykov, *Nuclear Waste Types and Sources*, in: *An Introd. to Nucl. Waste Immobil.*, Elsevier, 2019: pp. 119–143. <https://doi.org/10.1016/B978-0-08-102702-8.00010-8>.
- [6] W.E. Lee, M.I. Ojovan, M.C. Stennett, N.C. Hyatt, Immobilisation of radioactive waste in glasses, glass composite materials and ceramics, *Adv. Appl. Ceram.* 105 (2006) 3–12. <https://doi.org/10.1179/174367606X81669>.
- [7] M.I. Ojovan, W.E. Lee, W. Lee, *An Introduction to Nuclear Waste Immobilisation*, Elsevier, 2005. <https://doi.org/10.1016/B978-0-08-044462-8.X5000-5>.
- [8] A.I. Orlova, M.I. Ojovan, *Ceramic Mineral Waste-Forms for Nuclear Waste Immobilization*, *Materials (Basel)*. 12 (2019) 2638. <https://doi.org/10.3390/ma12162638>.
- [9] C.M. Jantzen, W.E. Lee, M.I. Ojovan, *Radioactive waste (RAW) conditioning, immobilization, and encapsulation processes and technologies: overview and advances*, in: *Radioact. Waste Manag. Contam. Site Clean-Up*, Elsevier, 2013: pp. 171–272. <https://doi.org/10.1533/9780857097446.1.171>.
- [10] C.M. Jantzen, *Historical development of glass and ceramic waste forms for high level radioactive wastes*, in: *Handb. Adv. Radioact. Waste Cond. Technol.*, Elsevier, 2011: pp. 159–172. <https://doi.org/10.1533/9780857090959.1.159>.
- [11] B.C. Chakoumakos, Systematics of the pyrochlore structure type, ideal A<sub>2</sub>B<sub>2</sub>X<sub>6</sub>Y, *J. Solid State Chem.* 53 (1984) 120–129. [https://doi.org/10.1016/0022-4596\(84\)90234-2](https://doi.org/10.1016/0022-4596(84)90234-2).
- [12] M.A. Subramanian, G. Aravamudan, G.V. Subba Rao, *Oxide pyrochlores — A review*,

- Prog. Solid State Chem. 15 (1983) 55–143. [https://doi.org/10.1016/00796786\(83\)90001-8](https://doi.org/10.1016/00796786(83)90001-8).
- [13] T. Subramani, A. Voskanyan, K. Jayanthi, M. Abramchuk, A. Navrotsky, A Comparison of Order-Disorder in Several Families of Cubic Oxides, *Front. Chem.* 9 (2021) 1–21. <https://doi.org/10.3389/fchem.2021.719169>.
- [14] S. Atiq, G.M. Mustafa, S. Naseem, S.K. Abbas, S.M. Ramay, A. Mahmood, Magneto-dielectric and ferroelectric tunability of multifunctional Ce-substituted neodymium zirconate pyrochlores, *Mater. Lett.* 243 (2019) 21–25. <https://doi.org/10.1016/j.matlet.2019.01.160>.
- [15] S. Saitzek, Z. Shao, A. Bayart, A. Ferri, M. Huvé, P. Roussel, R. Desfeux, Ferroelectricity in  $\text{La}_2\text{Zr}_2\text{O}_7$  thin films with a frustrated pyrochlore-type structure, *J. Mater. Chem. C* 2 (2014) 4037–4043. <https://doi.org/10.1039/c4tc00207e>.
- [16] D. Ai, J. Xu, C. Huang, W. Zhou, L. Zhao, J. Sun, Q. Wang, Synthesis and magnetoelectric properties of multiferroic composites of lead lanthanum zirconate titanate and mesoporous cobalt ferrite, *Scr. Mater.* 136 (2017) 29–32. <https://doi.org/10.1016/j.scriptamat.2017.04.003>.
- [17] J.E. Greedan, N.P. Raju, M.A. Subramanian, Structure and magnetic properties of the pyrochlore  $\text{Sc}_2\text{Mn}_2\text{O}_7$ , *Solid State Commun.* 99 (1996) 399–402. [https://doi.org/10.1016/0038-1098\(96\)00295-5](https://doi.org/10.1016/0038-1098(96)00295-5).
- [18] Z. Wang, G. Zhou, D. Jiang, S. Wang, Recent development of  $\text{A}_2\text{B}_2\text{O}_7$  system transparent ceramics, *J. Adv. Ceram.* 7 (2018) 289–306. <https://doi.org/10.1007/s40145-018-0287-z>.
- [19] X.-L. Xia, Z.-G. Liu, J.-H. Ouyang, Y. Zheng, Preparation, Structural Characterization, and Enhanced Electrical Conductivity of Pyrochlore-type  $(\text{Sm}_{1-x}\text{Eu}_x)_2\text{Zr}_2\text{O}_7$  Ceramics, *Fuel Cells* 12 (2012) 624–632. <https://doi.org/10.1002/fuce.201200015>.
- [20] F.X. Zhang, M. Lang, R.C. Ewing, Atomic disorder in  $\text{Gd}_2\text{Zr}_2\text{O}_7$  pyrochlore, *Appl. Phys. Lett.* 106 (2015) 191902. <https://doi.org/10.1063/1.4921268>.
- [21] H.C. Gupta, J. Singh, S. Kumar, Karandeep, N. Rani, A lattice dynamical investigation of the Raman and the infrared frequencies of the  $\text{Dy}_2\text{Ti}_2\text{O}_7$  pyrochlore spin ice compound, *J. Mol. Struct.* 937 (2009) 136–138. <https://doi.org/10.1016/j.molstruc.2009.08.027>.
- [22] L. Kong, I. Karatchevtseva, D.J. Gregg, M.G. Blackford, R. Holmes, G. Triani,  $\text{Gd}_2\text{Zr}_2\text{O}_7$  and  $\text{Nd}_2\text{Zr}_2\text{O}_7$  pyrochlore prepared by aqueous chemical synthesis, *J. Eur. Ceram. Soc.* 33 (2013) 3273–3285. <https://doi.org/10.1016/j.jeurceramsoc.2013.05.011>.

- [23] J. Lian, K.B. Helean, B.J. Kennedy, L.M. Wang, A. Navrotsky, R.C. Ewing, Effect of structure and thermodynamic stability on the response of lanthanide stannate pyrochlores to ion beam irradiation, *J. Phys. Chem. B.* 110 (2006) 2343–2350. <https://doi.org/10.1021/jp055266c>.
- [24] K.E. Sickafus, R.W. Grimes, J.A. Valdez, A. Cleave, M. Tang, M. Ishimaru, S.M. Corish, C.R. Stanek, B.P. Uberuaga, Radiation-induced amorphization resistance and radiation tolerance in structurally related oxides, *Nat. Mater.* 6 (2007) 217–223. <https://doi.org/10.1038/nmat1842>.
- [25] A.F. Fuentes, S.M. Montemayor, M. Maczka, M. Lang, R.C. Ewing, U. Amador, A Critical Review of Existing Criteria for the Prediction of Pyrochlore Formation and Stability, *Inorg. Chem.* 57 (2018) 12093–12105. <https://doi.org/10.1021/acs.inorgchem.8b01665>.
- [26] J. Shamblin, C.L. Tracy, R.C. Ewing, F. Zhang, W. Li, C. Trautmann, M. Lang, Structural response of titanate pyrochlores to swift heavy ion irradiation, *Acta Mater.* 117 (2016) 207–215. <https://doi.org/10.1016/j.actamat.2016.07.017>.
- [27] M.K. Patel, V. Vijayakumar, D.K. Avasthi, S. Kailas, J.C. Pivin, V. Grover, B.P. Mandal, A.K. Tyagi, Effect of swift heavy ion irradiation in pyrochlores, *Nucl. Instruments Methods Phys. Res. Sect. B Beam Interact. with Mater. Atoms.* 266 (2008) 2898–2901. <https://doi.org/10.1016/j.nimb.2008.03.135>.
- [28] G. Sattonnay, S. Moll, L. Thomé, C. Decorse, C. Legros, P. Simon, J. Jagielski, I. Jozwik, I. Monnet, Phase transformations induced by high electronic excitation in ion-irradiated  $Gd_2(Zr_xTi_{1-x})_2O_7$  pyrochlores, *J. Appl. Phys.* 108 (2010) 103512. <https://doi.org/10.1063/1.3503452>.
- [29] M. Jafar, S.B. Phapale, B.P. Mandal, M. Roy, S.N. Achary, R. Mishra, A.K. Tyagi, Effect of temperature on phase evolution in  $Gd_2Zr_2O_7$ : A potential matrix for nuclear waste immobilization, *J. Alloys Compd.* 867 (2021) 159032. <https://doi.org/10.1016/j.jallcom.2021.159032>.
- [30] C.R. Wiebe, A.M. Hallas, Frustration under pressure: Exotic magnetism in new pyrochlore oxides, *APL Mater.* 3 (2015) 041519. <https://doi.org/10.1063/1.4916020>.
- [31] J. Shamblin, C.L. Tracy, R.C. Ewing, F. Zhang, W. Li, C. Trautmann, M. Lang, Structural response of titanate pyrochlores to swift heavy ion irradiation, *Acta Mater.* 117 (2016) 207–215. <https://doi.org/10.1016/j.actamat.2016.07.017>.
- [32] G.J. McCarthy, Divalent europium compounds in the systems Eu--Mo--O and Eu--W--O, *Mater. Res. Bull.* 6 (1971) 31–39. [https://doi.org/10.1016/0025-5408\(71\)90156-5](https://doi.org/10.1016/0025-5408(71)90156-5).

- [33] M. Pokhrel, S.K. Gupta, K. Wahid, Y. Mao, Pyrochlore Rare-Earth Hafnate  $\text{RE}_2\text{Hf}_2\text{O}_7$  (RE=La and Pr) Nanoparticles Stabilized by Molten-Salt Synthesis at Low Temperature, *Inorg. Chem.* 58 (2019) 1241–1251. <https://doi.org/10.1021/acs.inorgchem.8b02728>.
- [34] G. Zhou, Z. Wang, B. Zhou, Y. Zhao, G. Zhang, S. Wang, Fabrication of transparent  $\text{Y}_2\text{Hf}_2\text{O}_7$  ceramics via vacuum sintering, *Opt. Mater. (Amst)*. 35 (2013) 774–777. <https://doi.org/10.1016/j.optmat.2012.09.016>.
- [35] Q. Feng, Q. Wang, Z. Zhang, Y. Xiong, H. Li, Y. Yao, X.-Z. Yuan, M.C. Williams, M. Gu, H. Chen, H. Li, H. Wang, Highly active and stable ruthenate pyrochlore for enhanced oxygen evolution reaction in acidic medium electrolysis, *Appl. Catal. B Environ.* 244 (2019) 494–501. <https://doi.org/10.1016/j.apcatb.2018.11.071>.
- [36] J. Kim, P.-C. Shih, K.-C. Tsao, Y.-T. Pan, X. Yin, C.-J. Sun, H. Yang, High-Performance Pyrochlore-Type Yttrium Ruthenate Electrocatalyst for Oxygen Evolution Reaction in Acidic Media, *J. Am. Chem. Soc.* 139 (2017) 12076–12083. <https://doi.org/10.1021/jacs.7b06808>.
- [37] G. Berti, S. Sanna, C. Castellano, J. Van Duijn, R. Ruiz-Bustos, L. Bordonali, G. Bussetti, A. Calloni, F. Demartin, L. Duò, A. Brambilla, Observation of Mixed Valence Ru Components in Zn Doped  $\text{Y}_2\text{Ru}_2\text{O}_7$  Pyrochlores, *J. Phys. Chem. C*. 120 (2016) 11763–11768. <https://doi.org/10.1021/acs.jpcc.5b12411>.
- [38] H. Kumar, A.K. Pramanik, Nonmagnetic Substitution in Pyrochlore Iridate  $\text{Y}_2(\text{Ir}_{1-x}\text{Ti}_x)_2\text{O}_7$ : Structure, Magnetism, and Electronic Properties, *J. Phys. Chem. C*. 123 (2019) 13036–13046. <https://doi.org/10.1021/acs.jpcc.9b02011>.
- [39] K. Matsuhira, M. Wakeshima, Y. Hinatsu, S. Takagi, Metal–Insulator Transitions in Pyrochlore Oxides  $\text{Ln}_2\text{Ir}_2\text{O}_7$ , *J. Phys. Soc. Japan*. 80 (2011) 094701. <https://doi.org/10.1143/JPSJ.80.094701>.
- [40] T.T. Zhang, K.W. Li, J. Zeng, Y.L. Wang, X.M. Song, H. Wang, Synthesis and structural characterization of a series of lanthanide stannate pyrochlores, *J. Phys. Chem. Solids*. 69 (2008) 2845–2851. <https://doi.org/10.1016/j.jpcs.2008.07.014>.
- [41] J. Feng, B. Xiao, Z.X. Qu, R. Zhou, W. Pan, Mechanical properties of rare earth stannate pyrochlores, *Appl. Phys. Lett.* 99 (2011) 201909. <https://doi.org/10.1063/1.3659482>.
- [42] J. Lian, L.M. Wang, S.X. Wang, J. Chen, L.A. Boatner, R.C. Ewing, Nanoscale manipulation of pyrochlore: New nanocomposite ionic conductors, *Phys. Rev. Lett.* 87 (2001) 3–6. <https://doi.org/10.1103/PhysRevLett.87.145901>.
- [43] S.X. Wang, B.D. Begg, L.M. Wang, R.C. Ewing, W.J. Weber, K. V. Govidan Kutty, Radiation stability of gadolinium zirconate: A waste form for plutonium disposition, *J.*

- Mater. Res. 14 (1999) 4470–4473. <https://doi.org/10.1557/JMR.1999.0606>.
- [44] J. Lian, X.T. Zu, K.V.G. Kutty, J. Chen, L.M. Wang, R.C. Ewing, R.C. Ewing, Ion-irradiation-induced amorphization of  $\text{La}_2\text{Zr}_2\text{O}_7$  pyrochlore, *Phys. Rev. B - Condens. Matter Mater. Phys.* 66 (2002) 541081–541085. <https://doi.org/10.1103/PhysRevB.66.054108>.
- [45] J. Lian, J. Chen, M. Wang, R.C. Ewing, J.M. Farmer, L.A. Boatner, B. Helean, Radiation-Induced amorphization of rare-Earth titanate pyrochlores, *Phys. Rev. B - Condens. Matter Mater. Phys.* 68 (2003) 1–9. <https://doi.org/10.1103/PhysRevB.68.134107>.
- [46] B.J. Kennedy, B.A. Hunter, C.J. Howard, Structural and Bonding Trends in Tin Pyrochlore Oxides, *J. Solid State Chem.* 130 (1997) 58–65. <https://doi.org/10.1006/jssc.1997.7277>.
- [47] K.M. Turner, C.L. Tracy, W.L. Mao, R.C. Ewing, Lanthanide stannate pyrochlores ( $\text{Ln}_2\text{Sn}_2\text{O}_7$ ; Ln = Nd, Gd, Er) at high pressure, *J. Phys. Condens. Matter.* 29 (2017) 504005. <https://doi.org/10.1088/1361-648X/aa9960>.
- [48] J.M. Farmer, L.A. Boatner, B.C. Chakoumakos, M.-H. Du, M.J. Lance, C.J. Rawn, J.C. Bryan, Structural and crystal chemical properties of rare-earth titanate pyrochlores, *J. Alloys Compd.* 605 (2014) 63–70. <https://doi.org/10.1016/j.jallcom.2014.03.153>.
- [49] S.T. Bramwell, Spin Ice State in Frustrated Magnetic Pyrochlore Materials, *Science* (5546)294 (2001) 1495–1501. <https://doi.org/10.1126/science.1064761>.
- [50] Y.H. Li, B.P. Uberuaga, C. Jiang, S. Choudhury, J.A. Valdez, M.K. Patel, J. Won, Y.Q. Wang, M. Tang, D.J. Safarik, D.D. Byler, K.J. McClellan, I.O. Usov, T. Hartmann, G. Baldinozzi, K.E. Sickafus, Role of antisite disorder on preamorphization swelling in titanate pyrochlores, *Phys. Rev. Lett.* 108 (2012) 1–5. <https://doi.org/10.1103/PhysRevLett.108.195504>.
- [51] K.E. Sickafus, L. Minervini, R.W. Grimes, J.A. Valdez, M. Ishimaru, F. Li, K.J. McClellan, T. Hartmann, Radiation tolerance of complex oxides, *Science* (5480)289 (2000) 748–751. <https://doi.org/10.1126/science.289.5480.748>.
- [52] R.C. Ewing, J. Lian, L.M. Wang, Ion beam-induced amorphization of the pyrochlore structure-type: A review, *Mater. Res. Soc. Symp. Proc.* 792 (2003) 37–48. <https://doi.org/10.1557/proc-792-r2.1>.
- [53] W.J. Weber, R.C. Ewing, L.-M. Wang, The radiation-induced crystalline-to-amorphous transition in zircon, *J. Mater. Res.* 9 (1994) 688–698. <https://doi.org/10.1557/JMR.1994.0688>.

- [54] J. Wen, C. Sun, P.P. Dholabhai, Y. Xia, M. Tang, D. Chen, D.Y. Yang, Y.H. Li, B.P. Uberuaga, Y.Q. Wang, Temperature dependence of the radiation tolerance of nanocrystalline pyrochlores  $A_2Ti_2O_7$  ( $A=Gd, Ho$  and  $Lu$ ), *Acta Mater.* 110 (2016) 175–184. <https://doi.org/10.1016/j.actamat.2016.03.025>.
- [55] F.X. Zhang, J.W. Wang, J. Lian, M.K. Lang, U. Becker, R.C. Ewing, Phase stability and pressure dependence of defect formation in  $Gd_2Ti_2O_7$  and  $Gd_2Zr_2O_7$  pyrochlores, *Phys. Rev. Lett.* 100 (2008) 2–5. <https://doi.org/10.1103/PhysRevLett.100.045503>.
- [56] F.X. Zhang, B. Manoun, S.K. Saxena, C.S. Zha, Structure change of pyrochlore  $Sm_2Ti_2O_7$  at high pressures, *Appl. Phys. Lett.* 86 (2005) 181906. <https://doi.org/10.1063/1.1925307>.
- [57] F.X. Zhang, M. Lang, Z. Liu, R.C. Ewing, Pressure-induced disordering and anomalous lattice expansion in  $La_2Zr_2O_7$  pyrochlore, *Phys. Rev. Lett.* 105 (2010) 1–4. <https://doi.org/10.1103/PhysRevLett.105.015503>.
- [58] D. Yang, Y. Xia, J. Wen, J. Liang, P. Mu, Z. Wang, Y. Li, Y. Wang, Role of ion species in radiation effects of  $Lu_2Ti_2O_7$  pyrochlore, *J. Alloys Compd.* 693 (2017) 565–572. <https://doi.org/10.1016/j.jallcom.2016.09.227>.
- [59] X. Lu, X. Shu, D. Shao, S. Chen, H. Zhang, X. Yuan, F. Chi, Radiation stability of  $Gd_2Zr_2O_7$  and  $Nd_2Ce_2O_7$  ceramics as nuclear waste forms, *Ceram. Int.* 44 (2018) 760–765. <https://doi.org/10.1016/j.ceramint.2017.09.244>.
- [60] K. Liu, K. Zhang, T. Deng, J. Zeng, B. Luo, H. Zhang, Grain size effects on the aqueous durability of  $Gd_2Zr_2O_7$  ceramics as high-level radioactive wastes matrix and its leaching mechanism, *Ceram. Int.* (2021) 1–11. <https://doi.org/10.1016/j.ceramint.2021.01.193>.
- [61] L. Zhou, Z. Huang, J. Qi, Z. Feng, D. Wu, W. Zhang, X. Yu, Y. Guan, X. Chen, L. Xie, K. Sun, T. Lu, Thermal-Driven Fluorite–Pyrochlore–Fluorite Phase Transitions of  $Gd_2Zr_2O_7$  Ceramics Probed in Large Range of Sintering Temperature, *Metall. Mater. Trans. A.* 47 (2016) 623–630. <https://doi.org/10.1007/s11661-015-3234-4>.
- [62] K. Liu, K. Zhang, T. Deng, W. Li, H. Zhang, Comparative study of irradiation effects on nanosized and microsized  $Gd_2Zr_2O_7$  ceramics, *Ceram. Int.* 46 (2020) 16987–16992. <https://doi.org/10.1016/j.ceramint.2020.03.283>.
- [63] S. Zinatloo-Ajabshir, M. Salavati-Niasari, A. Sobhani, Z. Zinatloo-Ajabshir, Rare earth zirconate nanostructures: Recent development on preparation and photocatalytic applications, *J. Alloys Compd.* 767 (2018) 1164–1185. <https://doi.org/10.1016/j.jallcom.2018.07.198>.
- [64] A. Panghal, P.K. Kulriya, Y. Kumar, F. Singh, N.L. Singh, Investigations of atomic

- disorder and grain growth kinetics in polycrystalline  $\text{La}_2\text{Zr}_2\text{O}_7$ , *Appl. Phys. A.* 125 (2019) 428. <https://doi.org/10.1007/s00339-019-2720-8>.
- [65] K. Liu, K. Zhang, T. Deng, B. Luo, H. Zhang, Heavy-ion irradiation effects of  $\text{Gd}_2\text{Zr}_2\text{O}_7$  nanocrystalline ceramics as nuclear waste immobilization matrix, *J. Nucl. Mater.* 538 (2020) 152236. <https://doi.org/10.1016/j.jnucmat.2020.152236>.
- [66] B. Paul, K. Singh, T. Jaroń, A. Roy, A. Chowdhury, Structural properties and the fluorite–pyrochlore phase transition in  $\text{La}_2\text{Zr}_2\text{O}_7$ : The role of oxygen to induce local disordered states, *J. Alloys Compd.* 686 (2016) 130–136. <https://doi.org/10.1016/j.jallcom.2016.05.347>.
- [67] T. Omata, S. Otsuka-Yao-Matsuo, Electrical Properties of Proton-Conducting  $\text{Ca}^{2+}$ Doped  $\text{La}_2\text{Zr}_2\text{O}_7$  with a Pyrochlore-Type Structure, *J. Electrochem. Soc.* 148 (2001) E252. <https://doi.org/10.1149/1.1369370>.
- [68] G. Ou, W. Liu, L. Yao, H. Wu, W. Pan, High conductivity of  $\text{La}_2\text{Zr}_2\text{O}_7$  nanofibers by phase control, *J. Mater. Chem. A.* 2 (2014) 1855–1861. <https://doi.org/10.1039/c3ta13465b>.
- [69] A. Chartier, C. Meis, W.J. Weber, L.R. Corrales, Theoretical study of disorder in Ti-substituted  $\text{La}_2\text{Zr}_2\text{O}_7$ , *Phys. Rev. B - Condens. Matter Mater. Phys.* 65 (2002) 1–11. <https://doi.org/10.1103/PhysRevB.65.134116>.
- [70] C.G. Liu, Y.H. Li, Y.D. Li, L.Y. Dong, J. Wen, D.Y. Yang, Q.L. Wei, P. Yang, First principle calculation of helium in  $\text{La}_2\text{Zr}_2\text{O}_7$ : Effects on structural, electronic properties and radiation tolerance, *J. Nucl. Mater.* 500 (2018) 72–80. <https://doi.org/10.1016/j.jnucmat.2017.12.024>.
- [71] N.. Kulkarni, S. Sampath, V. Venugopal, Preparation and characterisation of Pu-pyrochlore:  $[\text{La}_{1-x}\text{Pu}_x]_2\text{Zr}_2\text{O}_7$  ( $x=0-1$ ), *J. Nucl. Mater.* 281 (2000) 248–250. [https://doi.org/10.1016/S0022-3115\(00\)00336-6](https://doi.org/10.1016/S0022-3115(00)00336-6).
- [72] M.K. Patel, V. Vijayakumar, S. Kailas, D.K. Avasthi, J.C. Pivin, A.K. Tyagi, Structural modifications in pyrochlores caused by ions in the electronic stopping regime, *J. Nucl. Mater.* 380 (2008) 93–98. <https://doi.org/10.1016/j.jnucmat.2008.07.007>.
- [73] X. Lu, X. Shu, S. Chen, K. Zhang, F. Chi, H. Zhang, D. Shao, X. Mao, Heavy-ion irradiation effects on  $\text{U}_3\text{O}_8$  incorporated  $\text{Gd}_2\text{Zr}_2\text{O}_7$  waste forms, *J. Hazard. Mater.* 357 (2018) 424–430. <https://doi.org/10.1016/j.jhazmat.2018.06.026>.
- [74] X. Shu, L. Fan, Y. Xie, W. Zhu, S. Pan, Y. Ding, F. Chi, Y. Wu, X. Lu, Alpha-particle irradiation effects on uranium-bearing  $\text{Gd}_2\text{Zr}_2\text{O}_7$  ceramics for nuclear waste forms, *J. Eur. Ceram. Soc.* 37 (2017) 779–785. <https://doi.org/10.1016/j.jeurceramsoc.2016.09>.

- 034.
- [75] B.P. Mandal, M. Pandey, A.K. Tyagi,  $Gd_2Zr_2O_7$  pyrochlore: Potential host matrix for some constituents of thorium based reactor's waste, *J. Nucl. Mater.* 406 (2010) 238–243. <https://doi.org/10.1016/j.jnucmat.2010.08.042>.
- [76] M. Lang, F.X. Zhang, R.C. Ewing, J. Lian, C. Trautmann, Z. Wang, Structural modifications of  $Gd_2Zr_{2-x}Ti_xO_7$  pyrochlore induced by swift heavy ions: Disordering and amorphization, *J. Mater. Res.* 24 (2009) 1322–1334. <https://doi.org/10.1557/jmr.2009.0151>.
- [77] G. Sattonnay, S. Moll, L. Thomé, C. Legros, M. Herbst-Ghysel, F. Garrido, J.M. Costantini, C. Trautmann, Heavy-ion irradiation of pyrochlore oxides: Comparison between low and high energy regimes, *Nucl. Instruments Methods Phys. Res. Sect. B Beam Interact. with Mater. Atoms.* 266 (2008) 3043–3047. <https://doi.org/10.1016/j.nimb.2008.03.161>.
- [78] S.C. Finkeldei, Pyrochlore as nuclear waste form: Actinide uptake and chemical stability, 2015. [http://www.iaea.org/inis/collection/NCLCollectionStore/\\_Public/47/066/47066665.pdf](http://www.iaea.org/inis/collection/NCLCollectionStore/_Public/47/066/47066665.pdf)
- [79] S.K. Gupta, M. Abdou, P.S. Ghosh, J.P. Zuniga, E. Manoharan, H.J. Kim, Y. Mao, On comparison of luminescence properties of  $La_2Zr_2O_7$  and  $La_2Hf_2O_7$  nanoparticles, *J. Am. Ceram. Soc.* 103 (2020) 235–248. <https://doi.org/10.1111/jace.16693>.